Electronic Supplementary Material (ESI) for Catalysis Science & Technology.

Unravelling the Role of Ceria in Improving the Stability of Mo_2C Based Catalyst for Steam Reforming of Dimethyl Ether

Jing-Hong Lian[a,b,c,d], Hong-Yi Tan[a,b,c*], Chang-Qing Guo[a,b,c,e], Li-Sha Shen[a,b,c], Zhuo-Xin Lu[a,b,c], Yan Shi[a,b,c], Chang-Feng Yan[a,b,c,d*]

This file includes:

Materials

The ammonium heptamolybdate ($(NH_4)_6Mo_7O_{24}•4H_2O$, AR), cerium nitrate ($Ce(NO_3)_3·6H_2O$, 99.95% metals basis) and commercial γ-Al_2O_3 (99.99% metals basis) were purchased from Shanghai Aladdin Biochemical Technology Co., Ltd. Anhydrous methanol (CH_3OH, AR, ≥99.5%) and anhydrous ethanol (CH_3CH_2OH, AR, ≥99.5%) was purchased from Tianjin Damao Chemical Reagent Factory. Ar (≥99.999%), Hydrogen (≥99.999%), O_2/Ar mixture gas (1 vol% O_2), CH_4/H_2 mixture gas (20 vol% CH_4) and Air (21%O_2+N_2) were supplied from Guangzhou Shengying Chemical Co. Ltd. Pure water (H_2O, ≥18.0 MΩ*cm) was made by the pure water system produced by Nanjing Yipu Yida Technology Development Co., Ltd in the laboratory. The pure water was applied to the preparation of catalysts and the steam reforming reactions.

Evaluation of catalytic performance

The performance and stability testing method of steam reforming of dimethyl ether (DME) is the same as our previous work.[1] The steam reforming of DME (SRD) reaction was conducted in the self-built experimental device, and the reactor was a quartz tube which had the inner diameter of 6mm. The reactor was loaded with a mixture of 0.6 g sample dispersed in 1.5 g granulated quartz sand. Before the performance testing, all the samples were pretreated under CH_4/H_2 (20% vol% CH_4) atmosphere (590 °C, 2 h). During the SRD reaction, water was injected into the reacting system after the preheater. In the performance test of steam reforming of methanol (SRM) reaction, the mixed solution of H_2O and methanol (the molar ratio was 1:1) was vaporized and sent into the reacting system after the preheater. Ar was used as the balanced gas in the system, and the weighted hourly space velocity (WHSV) was 5500 $(ml·g·h)^{-1}$. After the reaction, the gas products were analyzed by a gas chromatography. The products of the reaction contained DME, methanol, H_2, CO, CO_2 and CH_4. The amount of product gas was measured according to the following equations: DME conversion $= \left(\frac{F_{DME,in} - F_{DME,out}}{F_{DME,in}}\right) * 100$, Methanol conversion

$= \left(\frac{F_{Methanol,in} - F_{Methanol,out}}{F_{Methanol,in}}\right) * 100$, $H_2\ Production\ Rate = \frac{F_{H_2}}{m_{cat}}$, and $H_2\ Yield = (\frac{F_{H_2}}{6 \times F_{DME,in}}) * 100$, $CO_2\ selectivity = \left(\frac{F_{CO_2}}{F_{CO_2} + F_{CO}}\right) * 100$, where $F_{DME,in}$ stands for the DME feed quantity (mol·min^{-1}), $F_{DME,out}$ stands for the DME outlet quantity (mol·min^{-1}), $F_{Methanol,in}$ stands for the methanol feed quantity (mol·min^{-1}), $F_{Methanol,out}$ stands for the methanol outlet flow (mol·min^{-1}), F_{H_2} stands for the flow rate of H_2 produced, F_{CO_2} stands for the flow rate of CO_2 produced, F_{CO} stands for the flow rate of CO produced, and m_{cat} is the weight of the catalyst.

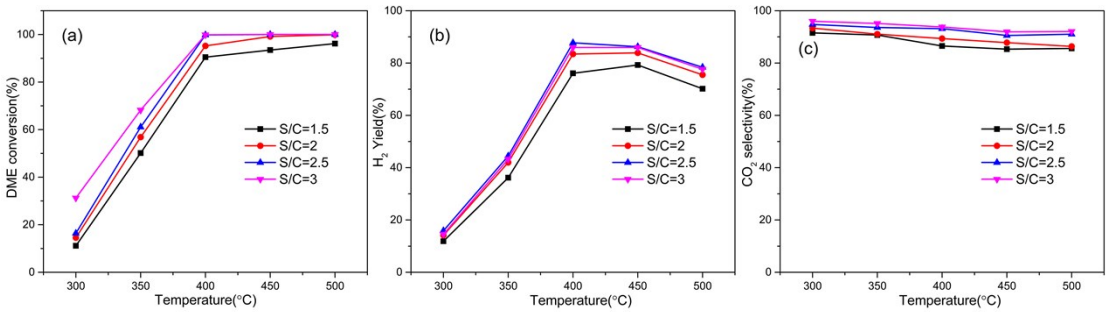

Fig. S1 Catalytic performance of Mo_2C-CeO_2/Al_2O_3 catalyst for DSR reaction at different S/C ratio: (a) DME conversion; (b) hydrogen yield; and (c) CO_2 selectivity.

SRD reaction is greatly affected by steam-to-carbon ratio (S/C). DME conversion and CO_2 selectivity increase with the increase of S/C at the same temperature. H_2 yield first increases and then decreases with the increasing of S/C. This is because more H_2O will promote the DME conversion, resulting in a higher H_2 yield. However, the excessive H_2O will dilute the reactants, leading to the decrease of the H_2 yield. Faungnawakij et al.[2] also confirmed that the high portion of steam can not only reduce the carbon deposition, but also promote the DME hydrolysis by shifting the equilibrium of hydrolysis. Based on the experimental results, we selected the optimal S/C as 2.5:1 in this paper.

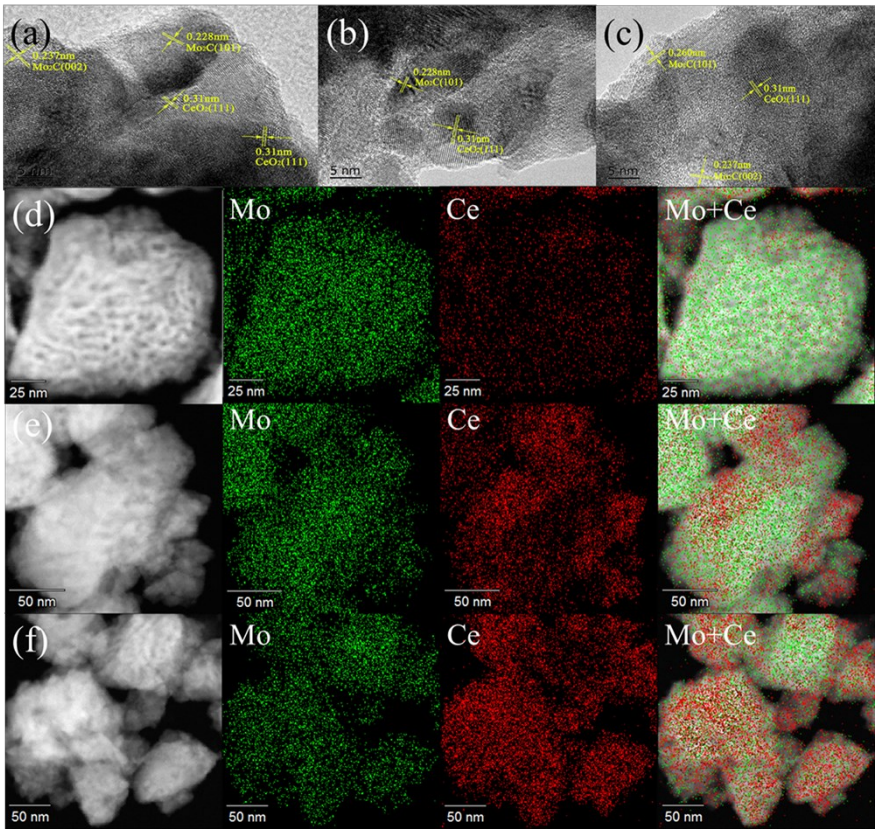

Fig. S2 TEM images of: (a) Mo_2C-CeO_2(0.05), (b) Mo_2C-CeO_2(0.1), (c) Mo_2C-CeO_2(0.3); and EDS mapping of: (d) Mo_2C-CeO_2(0.05), (e) Mo_2C-CeO_2(0.1), (f) Mo_2C-CeO_2(0.3).

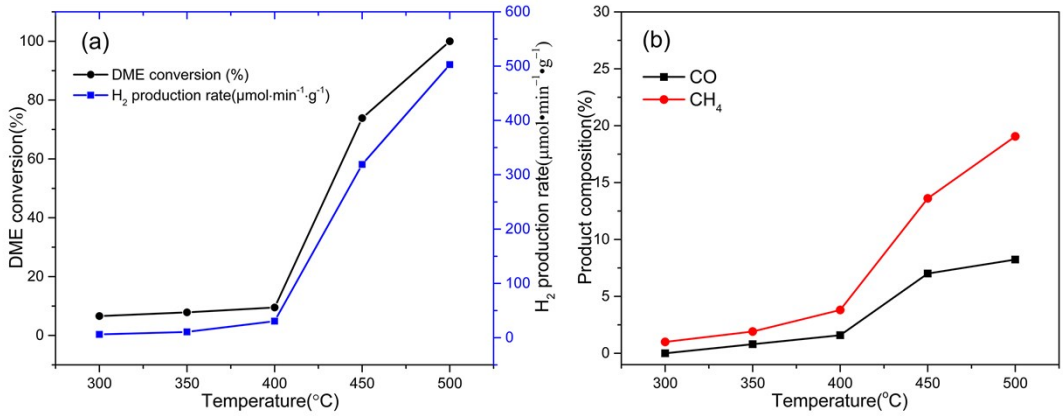

Fig. S3 Catalytic performance of CeO_2/Al_2O_3 catalyst for DSR reaction: (a) DME conversion and H_2 production rate; (b) Product composition of CO and CH_4. (Reaction conditions: atmosphere pressure; S/C =2.5:1; WHSV= 5500 $(ml \cdot g \cdot h)^{-1}$; 300-500 °C; carrier gas: Ar).

The results in Fig. S3 (a) substantiate the low activity of CeO_2/Al_2O_3 catalyst below 400°C; and the product composition of byproducts in (b) prove that large quantities of CO and CH_4 are generated when the temperatures are above 400 °C.

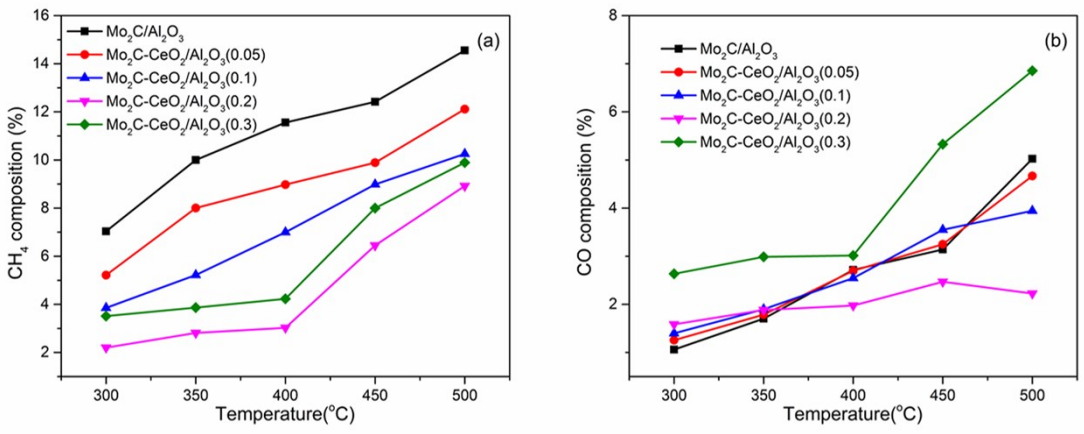

Fig. S4 Production of CH_4 and CO byproducts over Mo_2C-CeO_2/Al_2O_3 catalysts with different Mo/Ce ratios.

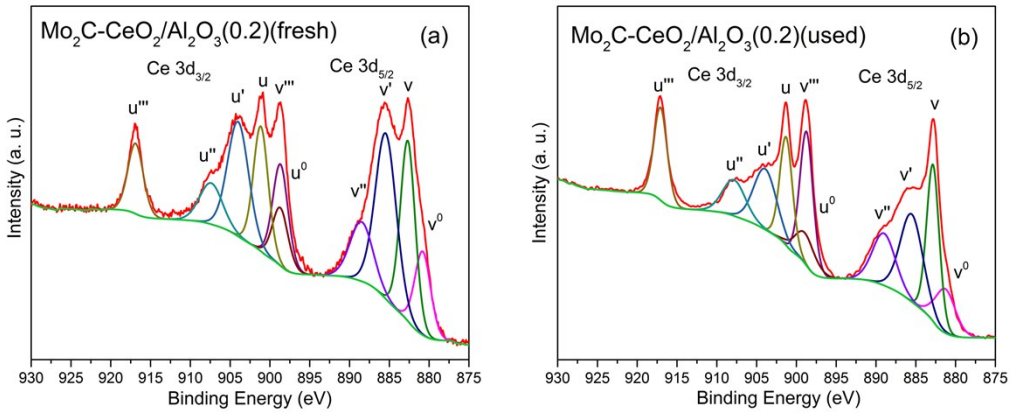

Fig. S5 Ce 3d spectra of: (a) Mo_2C-CeO_2/Al_2O_3(0.2)(fresh); and (b) Mo_2C-CeO_2/Al_2O_3(0.2)(used).

Ce 3d region of CeO_2 is composed of ten peaks, which belongs to Ce^{4+} (v, v'', v''', u, u'' and u''',) and Ce^{3+} (v^0 and v', u^0 and u') contributions.[3] XPS results prove the simultaneous existence of redox pair of Ce^{4+} and Ce^{3+} in Mo_2C-CeO_2/Al_2O_3(0.2) catalysts before and after the reaction, and the content of Ce^{3+} ($Ce^{3+}/(Ce^{3+}+Ce^{4+})$) is 47.6% and 40.2%, respectively.

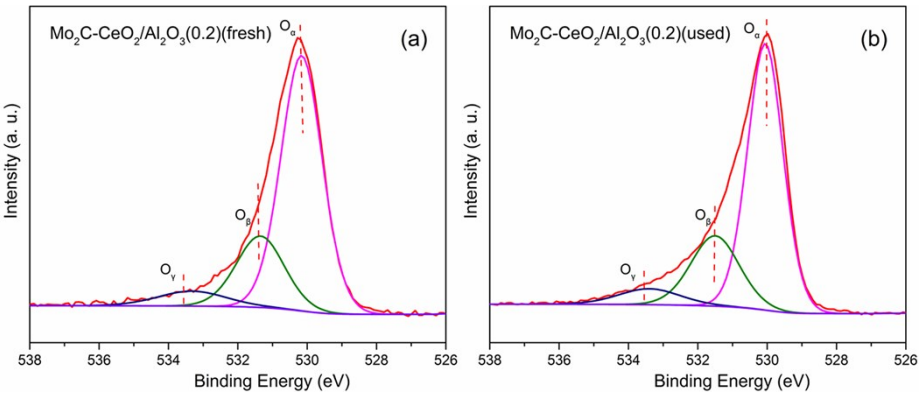

Fig. S6 O1s spectra of (a) Mo_2C-CeO_2/Al_2O_3(0.2)(fresh); (b) Mo_2C-CeO_2/Al_2O_3(0.2)(used).

Three kinds of surface oxygen species on the catalyst surface are detected and can be classified as O_α, O_β and O_γ species: O_α refer to lattice oxygen species, O_β and O_γ species could be assigned to adsorbed hydroxyl and water species, respectively.[4] The quantity of active surface oxygen species of Mo_2C-CeO_2/Al_2O_3(0.2) (fresh) and Mo_2C-CeO_2/Al_2O_3(0.2)(used) are 33.9% and 38.7% respectively, indicating that there are abundant active oxygen species on both fresh and used Mo_2C-CeO_2/Al_2O_3(0.2) catalysts.

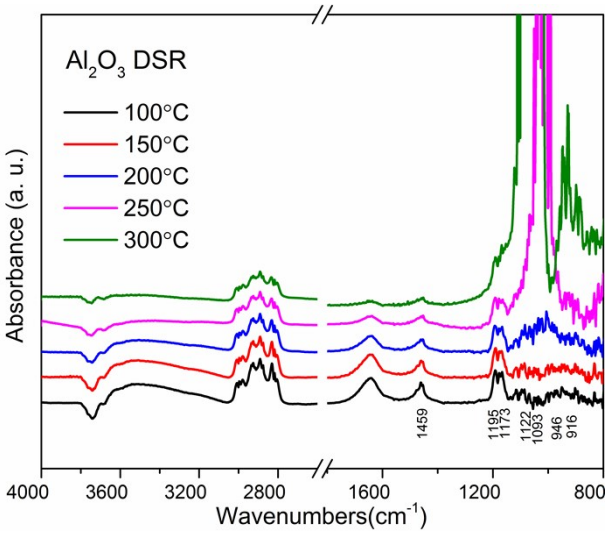

Fig. S7 In-situ DRIFTS of DSR reactions over Al_2O_3 catalyst at 100 °C and 400 °C.

The SRD consists of DME hydrolysis and the consequent SRM. Therefore, in situ DRIFTS study of DME hydrolysis over pure Al_2O_3 catalyst was also performed. After the reactants are introduced into the reaction chamber, the characteristic peaks assigned to DME are observed at 100 °C with no characteristic peaks of methanol or methoxy. When the temperature increases to 250 °C and 300 °C, there are strong characteristic peaks attributed to v_s(C-O) of methanol or methoxy at 1100cm^{-1}-1000cm^{-1} at the wavenumber's region, which is the evidence that the DME hydrolysis occurred over Al_2O_3 catalyst. However, the v_s(C-O) is not detected in the DRIFTS spectrum of SRD reaction, which is speculated that the methanol or methoxy intermediate is consumed by the methanol steam reforming reaction as soon as it was generated, and the remaining methanol or methoxy is lower than the detection limit of in situ DRIFTS.

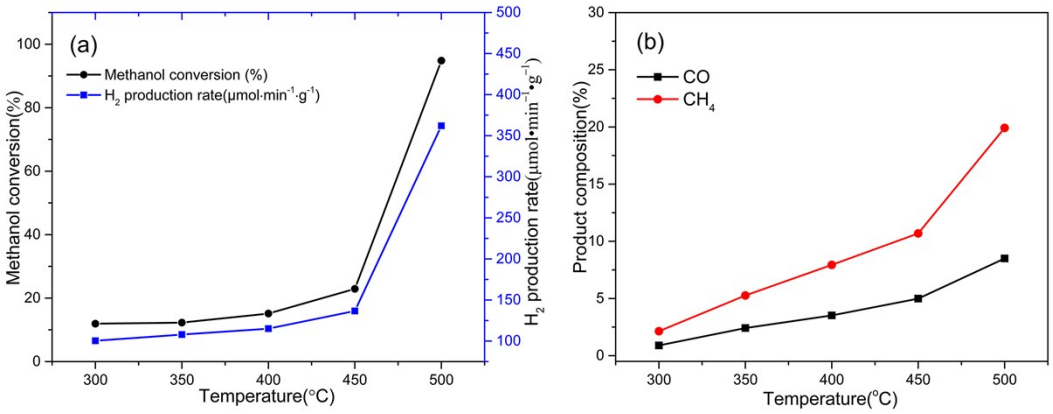

Fig. S8 Catalytic performance of CeO_2 catalyst for SRM reaction: (a) Methanol conversion and H_2 production rate; (b) Product composition of CO and CH_4. (Reaction conditions: atmospheric pressure; H_2O/Methanol = 1:1; WHSV= 5500 $(ml \cdot g \cdot h)^{-1}$; 300-500 °C; carrier gas: Ar).

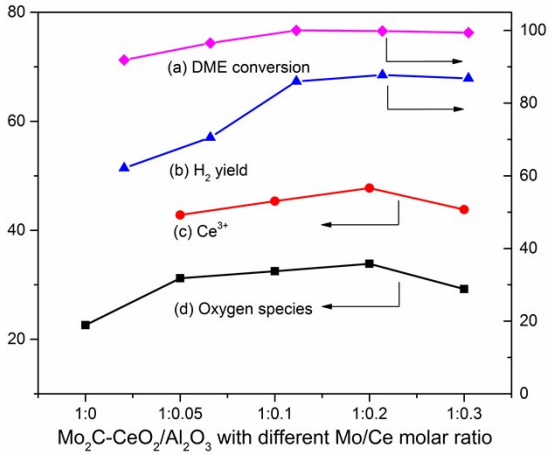

Fig. S9 Characteristic of Mo_2C-CeO_2/Al_2O_3 with different Mo/Ce ratios: (a) Ce^{3+} concentration; (b) active oxygen species; and catalytic performance of Mo_2C-CeO_2/Al_2O_3 at 400 °C with different Mo/Ce ratios: (c) DME conversion; (d) H_2 yield.

Table S1 Peak position and assignment of DME related species.[5]

Dimethyl Ether					
$v_{as}(CH_3)$	$2\delta_s(CH_3)$	$v_s(CH_3)$	$\delta(CH_3)$	v_{as}(C-O-C)	v_s(C-O-C)
2979 cm^{-1}, 2928 cm^{-1}	2891 cm^{-1}	2834 cm^{-1}, 2812 cm^{-1}	1459 cm^{-1}	1195 cm^{-1}, 1173 cm^{-1}	1117 cm^{-1}, 1093 cm^{-1}

Table S2 Peak position and assignment of Methanol related species.[6]

Methanol						
v_s(O-H)	Gaseous methanol	$v_{as}(CH_3)$	$v_s(CH_3)$	$2\delta_s(CH_3)$	$\delta(CH_3)$	v_s(C-O)
3750-3600 cm^{-1}	2865cm^{-1}	2972 cm^{-1}	2922 cm^{-1}	2843 cm^{-1}, 2827 cm^{-1}	1455 cm^{-1}	1056 cm^{-1}, 1032 cm^{-1}, 1011 cm^{-1}

Table S3 Assignment of steam reforming related intermediate species and products.

Formate			Methyl formate	CO	CO_2	Methane
Bidentate formate		Monodentate formate				
$v_{as}(OCO)$	$v_s(OCO)$	$v_s(OCO)$	v_s(C=O)			
1551 cm^{-1}, 1562 cm^{-1}	1360 cm^{-1}, 1310 cm^{-1}	1215 cm^{-1}	1713 cm^{-1}	2177 cm^{-1}, 2122 cm^{-1}	2363 cm^{-1}, 2338 cm^{-1}	3015 cm^{-1}

References

[1] J. H. Lian, H. Y. Tan, C. Q. Guo, Z. D. Wang, Y. Shi, Z. X. Lu, L. S, Shen, C. F. Yan, *Int. J. Hydrogen Energy* 2020**, 45**, 31523-31537.

[2] K. Faungnawakij, R. Kikuchi, T. Matsui, T. Fukunaga, K. Eguchii, *Appl. Catal. A* 2007, **333**, 114-121.

[3] a) J. Liu, Y. Du, J. Liu, Z. Zhao, K. Cheng, Y. Chen, Y. Wei, W. Song, X. Zhang, *Appl. Catal. B* 2017, **203**, 704-714; b) Z. Ferencz, A. Erdőhelyi, K. Baán, A. Oszkó, L. Óvári, Z. Kónya, C. Papp, H.P. Steinrück, J. Kiss, *ACS Catal.* 2014, **4**, 1205-1218; c) X. Yan, T. Hu, P. Liu, S. Li, B. Zhao, Q. Zhang, W. Jiao, S. Chen, P. Wang, J. Lu, L. Fan, X. Deng, Y.-X. Pan, *Appl. Catal. B* 2019, **246**, 221-231.

[4] S. Turczyniak, D. Teschner, A. Machocki, S. Zafeiratos, *J. Catal.* 2016, **340**, 321-330.

[5] a) C. Ledesma, U.S. Ozkan, J. Llorca, *Appl. Catal. B* 2011,**101**, 690-697; b) L. Yao, X. Shen, Y. Pan, Z. Peng, *Energy Fuels* 2020, **34,** 8635-8643.

[6] a) X. Yang, Y. Wei, Y. Su, L. Zhou, *Fuel Process. Technol.* 2010, **91**, 1168-1173; b) V.P. Santos, B. van der Linden, A. Chojecki, G. Budroni, S. Corthals, H. Shibata, G.R. Meima, F. Kapteijn, M. Makkee, J. Gascon, *ACS Catal.* 2013, **3**, 1634-1637; c) Z. Wu, M. Li, D.R. Mullins, S.H. Overbury, *ACS Catal.* 2012, **2**, 2224-2234; d) Z. Liu, S. Yao, A. Johnston-Peck, W. Xu, J.A. Rodriguez, S.D. Senanayake, *Catal. Today* 2018, **311**, 74-80.